Global Biogeochemical Cycles

Supporting Information for

Nitrogen biogeochemistry of adjacent mesoscale eddies in the North Pacific Subtropical Gyre

Mengyang Zhou[1], Julie Granger[1], Cesar B. Rocha[2], Samantha A. Siedlecki[1], Benedetto Barone[3], Angelicque E. White[3]

[1]Department of Marine Sciences, University of Connecticut, Groton, CT 06340, USA

[2]Instituto Oceanográfico, Universidade de São Paulo, São Paulo, SP 05508-120, Brasil

[3]Department of Oceanography, University of Hawai'i at Mānoa, Honolulu, HI 96822, USA

Corresponding author: Mengyang Zhou (mengyang.zhou2024@gmail.com)

Contents of this file

Introduction

This file contains further detailed information on the calculation of eddy nonlinearity (Text S1), and inferences of nitrate $\delta^{15}N_{NO3}$ supply to the euphotic zone (Text S2; Table S1), and corresponding supplementary figures S1 to S6.

Text S1. Calculation of eddy nonlinearity

Eddy nonlinearity is defined as the ratio of rotational fluid speed, *U*, to translation speed, *c* (Chelton et al., 2007, 2011). The rotational speeds of the cyclonic and anticyclonic eddies were calculated at each depth as the tangential velocity (calculated from ADCP measurements) at the eddy core edge (Chaigneau et al., 2011). The eddy core edge is defined by the radius of the best fit circle corresponding to the contour of maximum circum-average speed in the newest AVISO+ Mesoscale Eddy trajectory Atlas Product (META3.2 Delayed Time all satellites version). The translation speeds over the period of ADCP measurements were calculated from the time series of the eddy cores positions in AVISO+ META3.2. Profiles of eddy nonlinearity are shown in Fig. S1.

Text S2. Inference of nitrate $\delta^{15}N_{NO3}$ supply to the euphotic zone

At a steady state, the euphotic zone is neither gaining nor losing nitrogen, such that the export of particulate nitrogen from the surface ocean should be balanced by the supply of new nitrogen when integrated over a sufficiently long time period (Eppley & Peterson, 1979). The dominant sources of new nitrogen to the euphotic zone are the upward flux of nitrate from the subsurface and biological N_2 fixation in surface waters. As such, the N isotopic composition of the sinking flux of particulate material recovered in shallow sediment traps should reflect the proportion of source endmembers contributing to new production at the surface. This isotopic mass balance model relies on the unique isotopic signals of the two endmembers. Organic matter produced via N_2 fixation has a low $\delta^{15}N$ ($\delta^{15}N_{N2-fix}$= −2 ‰ to 0 ‰; Carpenter et al., 1997; Minagawa & Wada, 1986), while subsurface ocean nitrate has a higher $\delta^{15}N$ ($\delta^{15}N_{NO3}$ = 2.1 ‰ to 5.5 ‰ herein). The fraction of export production fueled by each can be estimated from the $\delta^{15}N$ values of the two sources ($\delta^{15}N_{NO3}$ and $\delta^{15}N_{N2-fix}$) relative to the $\delta^{15}N$ of sinking PO N ($\delta^{15}N_{PON}$). The fractional contribution of newly fixed nitrogen to the export production (f_{N2-fix}) is expressed as follows:

$$\delta^{15}N_{PON} = f_{N2-fix}\left(\delta^{15}N_{N2-fix}\right) + \left(1 - f_{N2-fix}\right)(\delta^{15}N_{NO3}) \quad (1)$$

Solving Eqn. 1 for f_{N2-fix},

$$f_{N2-fix} = (\delta^{15}N_{PON} - \delta^{15}N_{NO3})/(\delta^{15}N_{N2-fix} - \delta^{15}N_{NO3}) \quad (2)$$

The $\delta^{15}N_{NO3}$ value of the nitrate supplied to the euphotic zone depends on the assumptions of the mechanisms of nitrate supply to the surface (Table S1):

(1) Assuming the $\delta^{15}N_{NO3}$ values are those of nitrate originated from the specific depth of 175 m, the resulting estimates of $f_{N2\text{-}fix}$ are 23 ± 4 % and -3 ± 1 % in the cyclone and anticyclone, respectively. If from 250 m, $f_{N2\text{-}fix}$ estimates are comparable between features, 29 ± 5 % and 33 ± 7 % in the cyclone and anticyclone, respectively – yet not entirely consistent with estimates at 175 m.

(2) If nitrate is supplied to the euphotic zone through isopycnal uplift (*aka*, eddy injection), the corresponding $\delta^{15}N_{NO3}$ values correspond to the depth integral of the concentration weighted $\delta^{15}N_{NO3}$ (Casciotti et al., 2008). Resulting estimates of $f_{N2\text{-}fix}$ are 25 ± 5 % and -3 ± 1 % in the cyclone and anticyclone, respectively, when integrating $\delta^{15}N_{NO3}$ from 150 to 175 m, and 27 ± 5 % and 29 ± 7 % when integrating over 150 - 250 m.

(3) If steady-state turbulent diffusion dominates the upward nitrate supply, the upwelled $\delta^{15}N_{NO3}$ can be calculated from vertical gradients in concentration of ^{15}N and ^{14}N in nitrate: $\delta^{15}N_{NO3} = ((d[^{15}N]/dz)/(d[^{14}N]/dz)/^{15}R_{air} - 1)*1000$, where $^{15}R_{air}$ is the $^{15}N/^{14}N$ ratio of N_2 gas in air (Casciotti et al., 2008). The concentration gradient from 175 m decreases to the surface for ^{14}N but increase for ^{15}N due to fractionation during assimilation – yielding an estimate for the $\delta^{15}N_{NO3}$ supply of 8.7 ± 0.3‰ and 4.6 ± 0.3‰ for the cyclone and anticyclone, respectively. Corresponding estimates of $f_{N2\text{-}fix}$ are 51 ± 7 % and 23 ± 6 %. Estimates considering N isotope gradients from 250 m to 150 m are complicated by the reversal in the direction of the ^{15}N gradient; we thus interpolate the gradient directly from 250 m to 150 m; estimates of the nitrate $\delta^{15}N_{NO3}$ supply based on gradient from 250 m to 150 m are 5.9 ± 0.3 ‰ and 6.1 ± 0.4 ‰ in the cyclone and anticyclone, respectively, resulting in $f_{N2\text{-}fix}$ estimates of 28 ± 5 % and 43 ± 8 %.

The range of estimates above is confounding. Notwithstanding the non-steady state nature of the system, a number of the scenarios tested above yield a higher contribution of N_2 fixation to the export flux in the cyclone than in the anticyclone – contradicting the incubation-based estimates that show substantially higher rates of N_2 fixation in the anticyclone (Dugenne et al., 2023). Estimates for a given nutrient supply mechanism are also highly sensitive to the depth presumed pertinent to these dynamics – rendering them exceedingly uncertain.

Table S1. Averaged $\delta^{15}N_{PON}$ of PON recovered in sediment traps and the corresponding $\delta^{15}N_{NO3}$ of the nitrate supplied to the euphotic zone under different assumed mechanisms of nitrate supply. The fraction of export production fueled by N_2 fixation ($f_{N2\text{-}fix}$) was calculated using Equation S2, assuming $\delta^{15}N_{N2\text{-}fix}$ = 0 ± 1‰. $\delta^{15}N_{PON}$ values were averaged over trap stations 1 and 2 for the cyclone, and trap stations 7 – 12 for the anticyclone. $\delta^{15}N_{NO3}$ values were averaged over hydrographic stations 11 and 12 for the cyclone, and hydrographic stations 6 – 9 for anticyclone (Fig. 1).

Nitrate supply	Mesoscale feature	$\delta^{15}N_{PON}$ (‰ vs. Air)	$\delta^{15}N_{NO3}$ (‰ vs. Air)	$f_{N2\text{-}fix}$ (%)
175 m	Cyclone	4.3 ± 0.2	5.6 ± 0.1	23 ± 4
	Anticyclone	3.5 ± 0.3	3.4 ± 0.2	-3 ± 1
250 m	Cyclone	4.3 ± 0.2	6.0 ± 0.2	29 ± 5
	Anticyclone	3.5 ± 0.3	5.2 ± 0.3	33 ± 7
Eddy injection 150 - 175 m	Cyclone	4.3 ± 0.2	5.7 ± 0.3	25 ± 5
	Anticyclone	3.5 ± 0.3	3.4 ± 0.3	-3 ± 1
Eddy injection 150 - 250 m	Cyclone	4.3 ± 0.2	5.9 ± 0.3	27 ± 5
	Anticyclone	3.5 ± 0.3	4.9 ± 0.4	29 ± 7
Diffusion 150 – 175 m	Cyclone	4.3 ± 0.2	8.7 ± 0.3	51 ± 7
	Anticyclone	3.5 ± 0.3	4.6 ± 0.3	23 ± 6
Diffusion 150 – 250 m	Cyclone	4.3 ± 0.2	5.9 ± 0.3	28 ± 5
	Anticyclone	3.5 ± 0.3	6.1 ± 0.4	43 ± 8

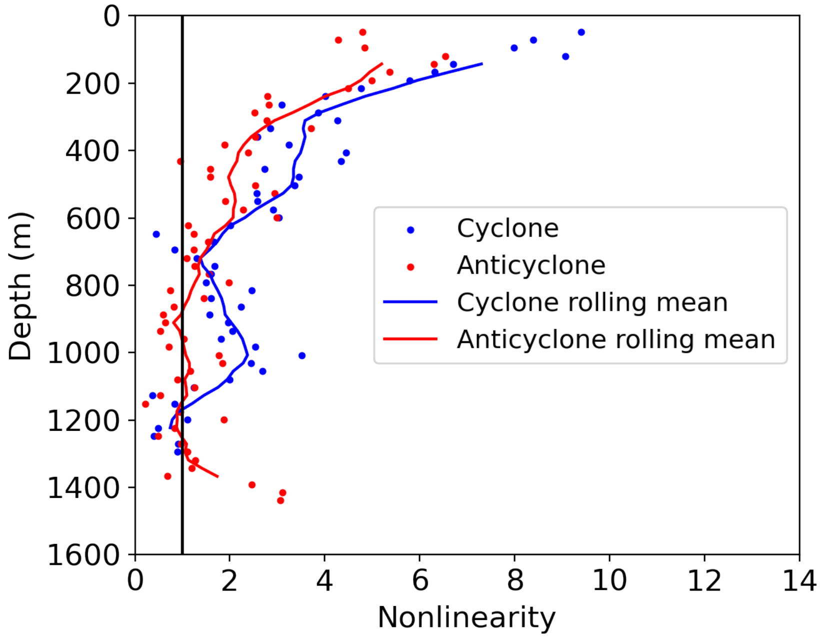

Figure S1. Nonlinearity of the cyclonic (blue) and anticyclonic (red) eddy. Solid lines are the rolling mean values. The black vertical line represents nonlinearity of 1.

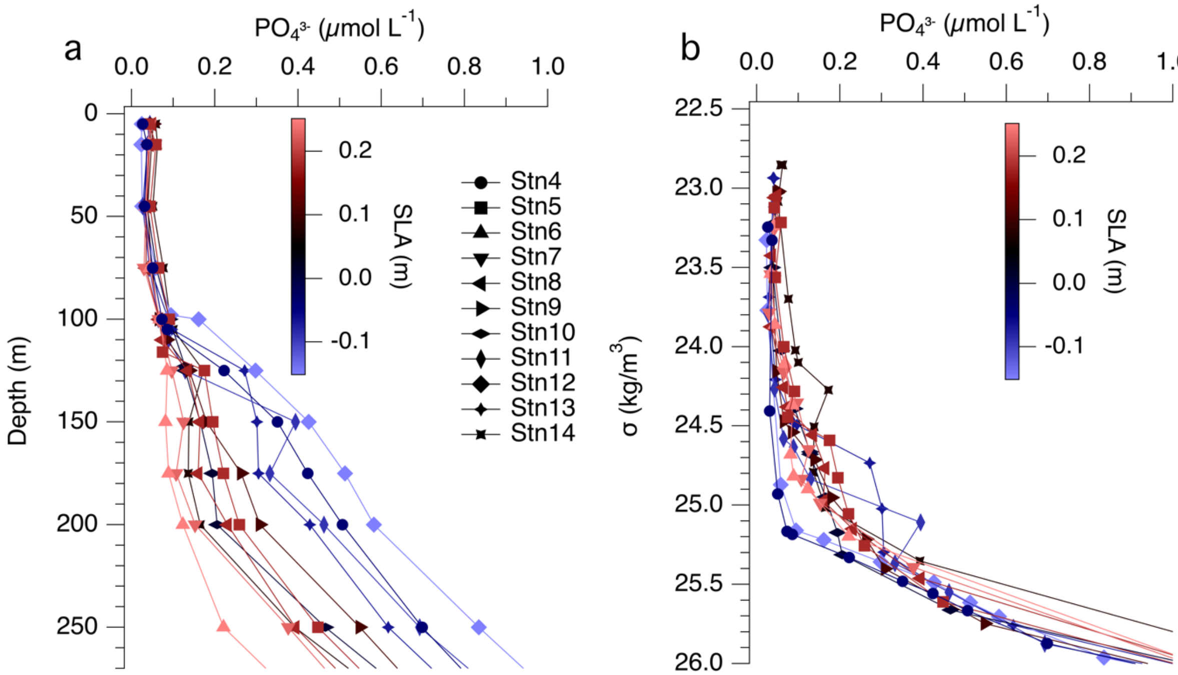

Figure S2. Shallow depth (a) and potential density (b) profiles of PO_4^{3-} concentration at stations along the hydrographic transect. Colors correspond to corrected sea level anomaly.

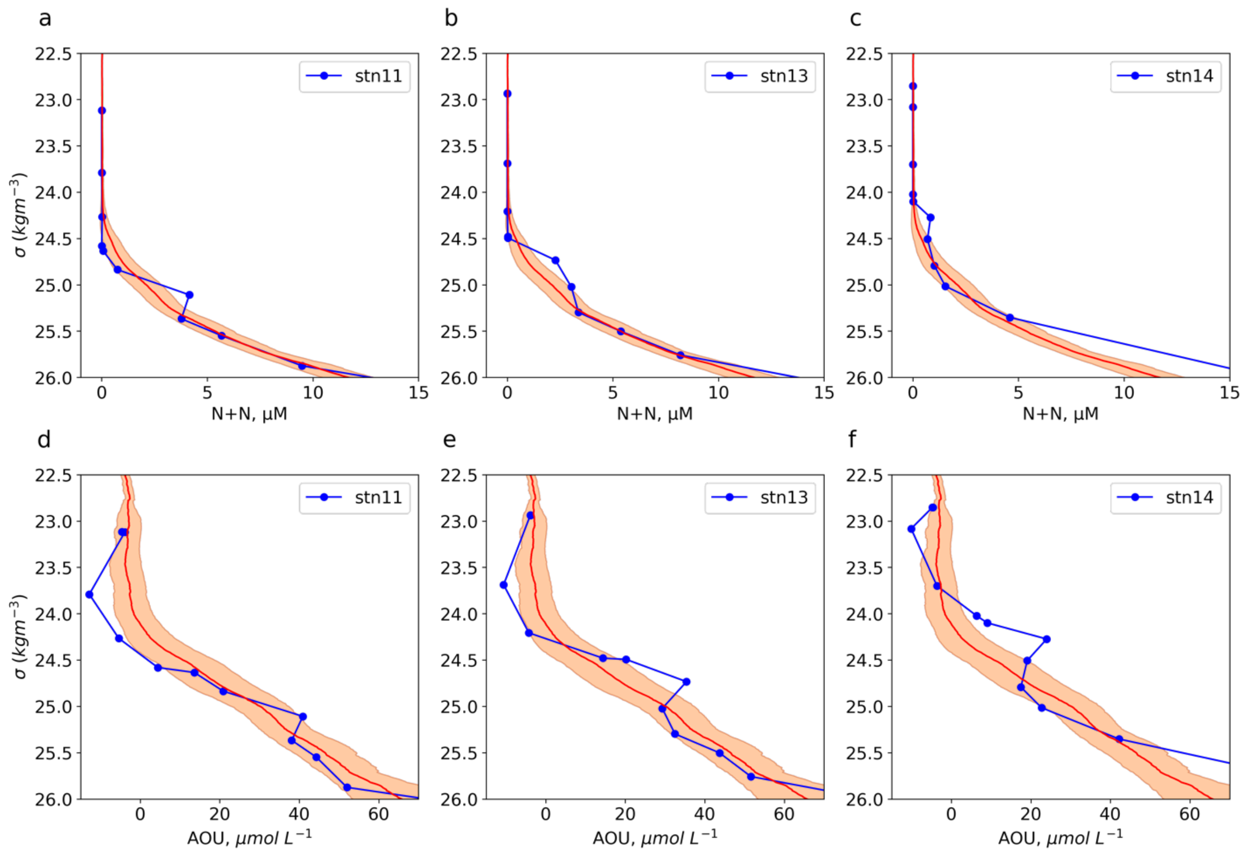

Figure S3. Potential density profiles of N+N and AOU concentrations at stations 11 (a, d), 13 (b, e) and 14 (c, f), relative to mean condition (red line) with standard deviation (shaded area) at Station ALOHA. The mean condition was calculated using the Hawaii Ocean Time-series observations (http://hahana.soest.hawaii.edu/hot/hot-dogs/).

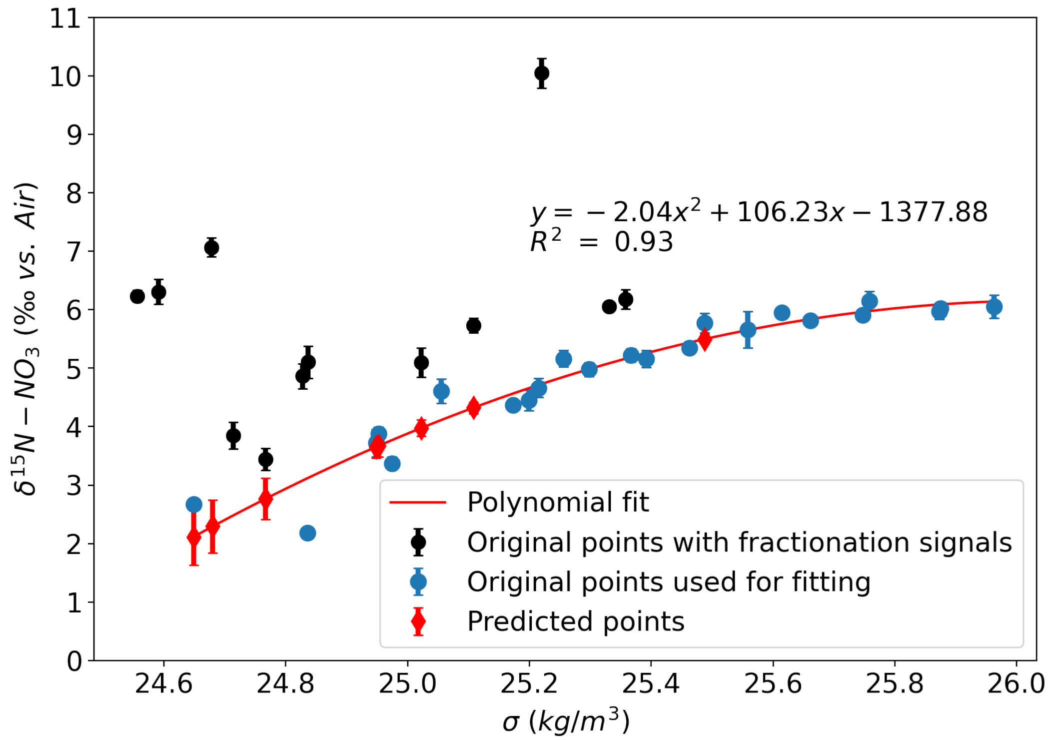

Figure S4. Measured and interpolated $\delta^{15}N_{NO3}$ values plotted against potential density. Measured values without fractionation signals (in blue) are used to fit a polynomial curve, from which $\delta^{15}N_{NO3}$ values at 150 m before fractionation were interpolated for each station (in red). Measured values with fractionation signals are shown in black.

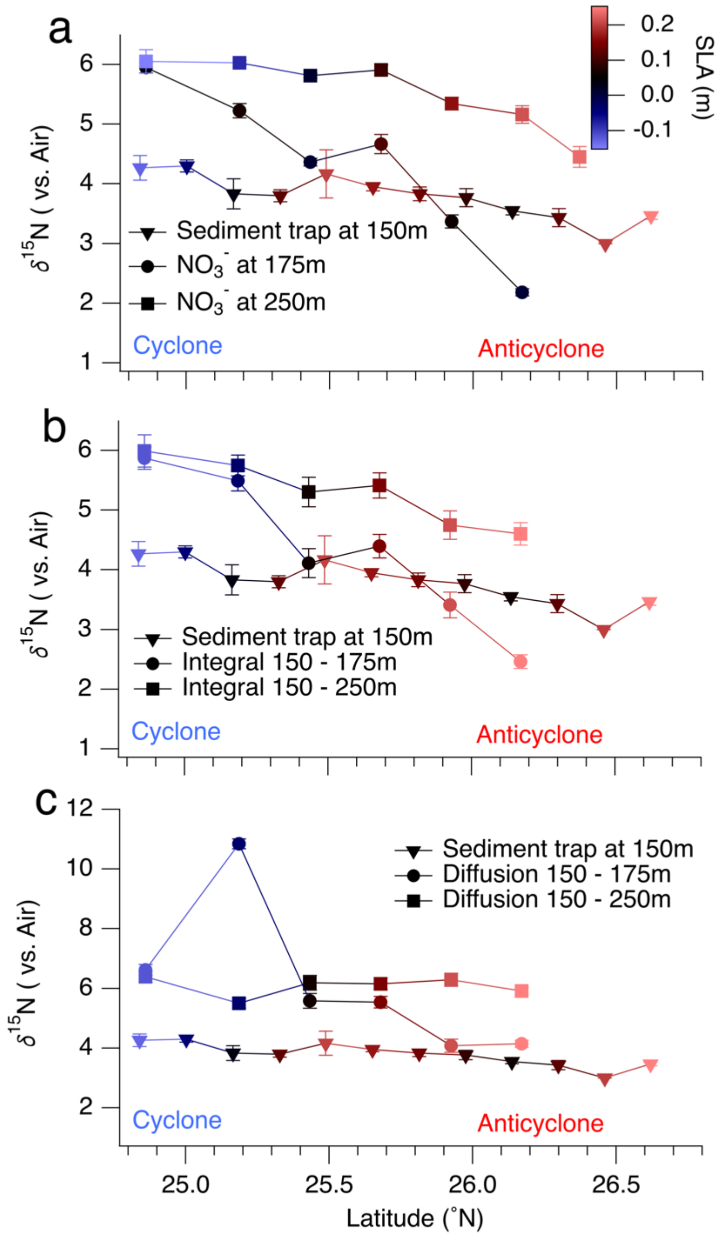

Figure S5. Sediment trap $\delta^{15}N_{PON}$ values and $\delta^{15}N_{NO3}$ values under different assumed mechanisms of nitrate supply to the euphotic zone: (a) at 175 m and 250 m, (b) eddy injection over 150 - 175 m and 150 – 250 m, and (c) diffusion over 150 - 175 m and 150 – 250 m, plotted against latitudes along the hydrographic transect. Colors represent corrected sea level anomaly. Error bars are the uncertainties from measurements for $\delta^{15}N_{PON}$ and $\delta^{15}N_{NO3}$ in (a). Errors were propagated during calculation of $\delta^{15}N_{NO3}$ in (b, c).

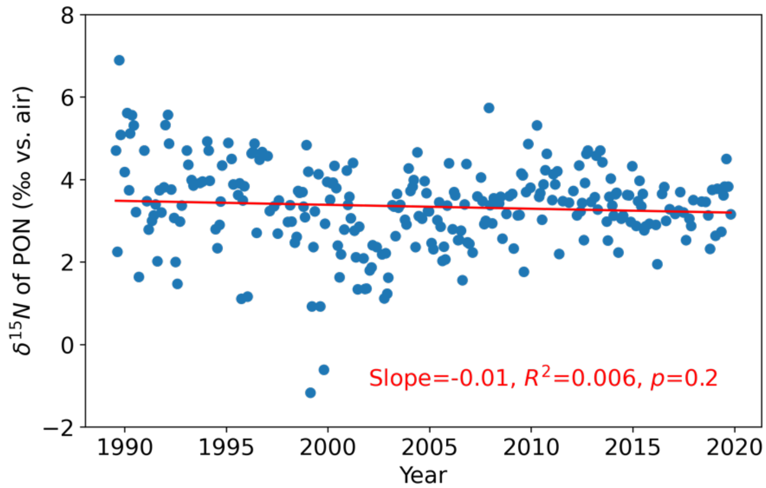

Figure S6. Time series of the $\delta^{15}N$ of particulate organic nitrogen (PON) collected in shallow sediment traps at Station ALOHA. The data are from The Hawaii Ocean Time-series observations (http://hahana.soest.hawaii.edu/hot/hot-dogs/).